JOURNAL OF GEOPHYSICAL RESEARCH, VOL. 103, NO. D22, PAGES 28,963–28,973, NOVEMBER 27, 1998

Active-layer thickness in north central Alaska: Systematic sampling, scale, and spatial autocorrelation

F. E. Nelson,[1] K. M. Hinkel,[2] N. I. Shiklomanov,[1] G. R. Mueller,[1] L. L. Miller,[2] and D. A. Walker[3]

Abstract. Active-layer thickness was determined in late August 1995 and 1996 at 100 m intervals over seven 1 km^2 grids in the Arctic Coastal Plain and Arctic Foothills physiographic provinces of northern Alaska. Collectively, the sampled areas integrate the range of regional terrain, soil, and vegetation characteristics in this region. Spatial autocorrelation analysis indicates that patterns of active-layer thickness are governed closely by topographic detail, acting through near-surface hydrology. On the coastal plain, maximum variability occurs at scales involving hundreds of meters, and patterns were similar in the two years. Substantially less spatial structure and interannual correspondence were found within the foothill sites, where high variability occurs over smaller distances. The divergence in patterns of thaw depth between the two provinces reflects the scale of local terrain features, which predetermines the effectiveness of fixed sampling intervals. Exploratory analysis should be performed to ascertain the scale(s) of maximum variability within representative areas prior to selection of sampling intervals and development of long-term monitoring programs.

1. Introduction

The active layer, a thickness of soil or other earth material above permafrost, experiences freezing and thawing on an annual basis. Given similar surface cover and soil properties, the active layer thins progressively toward the poles in response to shorter, cooler summers. Under a warming climate, such as that predicted by many general circulation models [*Manabe et al.*, 1991; *Cubasch et al.*, 1992; *Murphy and Mitchell*, 1994], the active layer could thicken and release water and carbon stored in the upper permafrost [*Hinzman and Kane*, 1992; *Anisimov et al.*, 1997; *Waelbroeck et al.*, 1997]. Additional direct effects include surface subsidence and thermokarst, which could have negative impacts on the landscape and infrastructure [*Nelson et al.*, 1993; *Williams*, 1995]. For these reasons, active-layer and permafrost dynamics are considered to be an integral component of Arctic ecosystems, and their effects are being incorporated in local, regional, and global models [*Waelbroeck*, 1993; *Savtchenko*, 1998].

Active-layer thickness varies both spatially and temporally, partly in response to air temperature. Although warmer summers are generally associated with thicker thawed layers at particular locations, this relation is not absolute because winter snow cover, summer rainfall, soil properties, and vegetation characteristics can influence thaw depth [e.g., *Smith*, 1975; *Goodrich*, 1982; *Hinkel et al.*, 1993; *Zhang et al.*, 1996b]. The depth of thaw can also vary substantially across small lateral distances. Because the flux of trace gases from the tundra to the atmosphere is related to the thickness of the active layer, the ability to assess the spatial heterogeneity of active-layer thickness is a critical component of efforts to estimate regional emissions of CO_2 and CH_4 in the Arctic [*Weller et al.*, 1995; *Nelson et al.*, 1997b]. Little is known, however, about variations of thaw depth over extensive areas that incorporate diverse surface and subsurface characteristics, particularly on an interannual basis.

Many strategies for calculating the thickness of the seasonally thawed layer have been developed, ranging from relatively simple analytic techniques to complex numerical modeling schemes. One of the most fundamental relations involved in assessing active-layer development is its proportionality with the square root of seasonal degree-days of thaw [e.g., *Jumikis*, 1977; *Hinkel and Nicholas*, 1995; *Nelson et al.*, 1997b]. Spatial integration is not straightforward, however, because many of the factors influencing thaw depth can vary over short lateral distances. Although substantial progress has been obtained recently [*Peddle and Franklin*, 1993; *Leverington and Duguay*, 1996; *McMichael et al.*, 1997], remote sensing has not yet provided an effective solution to the general problem of treating spatial variations of thaw depth. Statistical analysis of data collected directly in the field is therefore currently the primary vehicle for addressing the spatial and temporal variability of active-layer thickness.

Nelson et al. [1997b] mapped variations in active-layer thickness over a 26,278 km^2 area in north central Alaska. Mean values of thaw depth in representative 1 ha land cover units were associated with temperature data, a topoclimatic index, and digital terrain and land cover maps to produce a spatial time series of active-layer thickness at weekly intervals. Errors in predicted values of active-layer thickness were less than 10% of measured averages in representative 1 km^2 units arrayed over the north-south extent of the mapped area, indicating that the controlling variables were specified effectively at the scale of the study. Although values used to represent the 90,000 m^2 map pixels reflect average conditions under specific land cover

[1]Department of Geography, University of Delaware, Newark.
[2]Department of Geography, University of Cincinnati, Cincinnati, Ohio.
[3]Institute of Arctic and Alpine Research, University of Colorado, Boulder.

Paper number 98JD00534.
0148-0227/98/98JD-00534$09.00

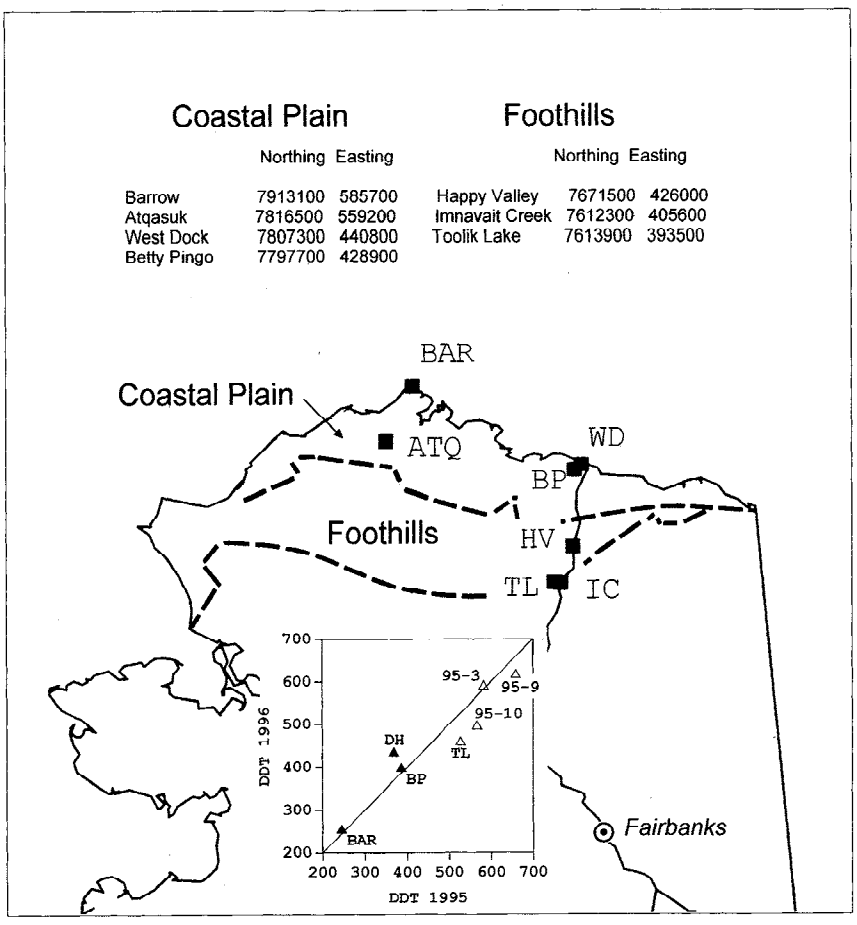

Figure 1. Locations of Arctic System Science (ARCSS) grids (squares) in north central Alaska. Numbers indicate southwest corners (universal transverse mercator (UTM) coordinates in meters, zone 6) of 1 km^2 ARCSS grids. Boundaries of *Wahrhaftig*'s [1965] Arctic Coastal Plain and Arctic Foothills physiographic provinces are indicated. Scattergram shows correspondence between sums of thawing degree-days in 1995 and 1996 (mid-June to mid-August) at sites within study area. Solid and open symbols represent coastal plain and foothills installations, respectively. Locations of temperature installations are provided by *Nelson et al.* [1997b, Figure 1].

categories, the maps provide no information about the variability of the depth of thaw within the component spatial units.

This study examines patterns of thaw depth within integrated mosaics of vegetation/soil associations representative of conditions in the Kuparuk River region of north central Alaska (Figure 1). Active-layer data collected from the 1 km^2 areas, used to validate the previous regional study [*Nelson et al.*, 1997b], are employed to identify factors that exert a strong influence on local thaw depth and to assess the adequacy of a systematic (fixed interval) sampling design used for multiple purposes in the Arctic Flux Study [*Weller et al.*, 1995].

2. Study Area and Field Procedures

It is currently unknown if systematic changes in Arctic ecosystems are occurring as part of ongoing, very long term landscape evolution or in response to climatic change. Repeated observations at permanent plots over long periods are required to detect and discern the reasons for change, and a series of seven surveyed and georeferenced 1 km^2 grids (Figure 1) was established in northern Alaska during the 1980s and 1990s for this purpose [*Walker and Walker*, 1991; *Walker*, 1997]. Five of the sites are adjacent to roads constructed in support of the Trans-Alaska Pipeline System (Betty Pingo, West Dock, Happy Valley, Toolik Lake, and Imnavait Creek) and represent a north-south transect along the axis of the Kuparuk River basin through the Arctic Coastal Plain and Arctic Foothills physiographic provinces [*Wahrhaftig*, 1965]. A second transect incorporates sites at Barrow and Atqasuk, approximately 150 km west of the Kuparuk transect. Together, these sites demonstrate the varied factors controlling and influencing patterns of summer thaw in the study area. Climatic conditions along the first transect were summarized by *Haugen and Brown* [1980], *Haugen* [1982], and *Zhang et al.* [1996a]. Aspects of Barrow's climate record have been treated by *Weller and Holmgren* [1974], *Haugen and Brown* [1980], and *Dutton and Endres* [1991]. Records at Atqasuk are very sparse prior to the 1990s [*Haugen et al.*, 1976]. On the basis of these limited data, *Haugen and Brown* [1980] discussed contrasts in the climatic regimes of Barrow and Atqasuk.

The grids at Barrow, Atqasuk, West Dock, and Betty Pingo are located in the Arctic Coastal Plain physiographic province [*Wahrhaftig*, 1965], in which major geomorphic, edaphic, and ecological variations are related to the presence of thaw-lake basins and ice-wedge polygons. The Happy Valley, Toolik

Lake, and Imnavait Creek grids are in the Arctic foothills physiographic province, where the existence of tundra tussocks, shallowly incised drainage channels known as "water tracks" [*Hastings et al.*, 1989], and abrupt changes in site exposure over small horizontal distances give rise to high-frequency variations in ecological and geomorphic parameters [*Nelson et al.*, 1997a].

Each of the grids used in this study consists of a square network of iron stakes located at 100 m horizontal intervals and surveyed to a high order of horizontal and vertical accuracy (±10 cm). Each grid is oriented along north–south/east–west axes and positioned with its southwest corner at a round universal transverse mercator (UTM) coordinate (Figure 1), allowing it to be located precisely for GIS and remote sensing work. Landscape-level databases have been collected for a wide variety of ecological data on the grids at Toolik Lake and Imnavait Creek. These grids were established under the R4D project funded by the Department of Energy in the mid-1980s [*Evans et al.*, 1989; *Walker et al.*, 1989; *Reynolds and Tenhunen*, 1996]. Grids at Atqasuk, Barrow, Betty Pingo, Happy Valley, and West Dock were installed for the Flux Study [*Weller et al.*, 1995], and landscape-level maps are in progress for these sites. The grids are referred to informally as the "ARCSS grids," for the National Science Foundation (NSF) Arctic System Science program, and form the core of the Circumpolar Active Layer Monitoring (CALM) program in Alaska [*Brown et al.*, 1997]. They were established to provide a basis for integrated, multidisciplinary work and correlations between variables at common sites located precisely with respect to external, three-dimensional coordinate systems.

A steel rod, graduated in centimeters, was used to determine the thickness of the thawed layer. Extensive testing with a Yellow Springs Instruments model 419 thermal probe [cf. *Mackay*, 1977, 1995] indicates that the depth at which resistance to probing was encountered corresponds closely to the position of the frost table. Measurements were made at each grid node on three or four dates during the summers of 1995 and 1996, which had very similar temperature regimes (Figure 1). On each probing date an 11 × 11 array of thaw depth data was collected near grid nodes at regular intervals of 100 m. Two measurements, each within 1 m of the stake location, were obtained at each of the 121 grid nodes, in accordance with established CALM/ITEX procedures [*Nelson et al.*, 1996]. The mean of these duplicate measurements was used in this analysis, which treats only end-of-season (middle to late August) values.

Some nodes on the grids are inaccessible on some occasions owing to, for example, deep standing water. This situation necessitated interpolation onto a regular lattice, which was accomplished using minimum curvature [*Smith and Wessel*, 1990]. The procedure provided an exact fit at locations for which data exist. Descriptive statistics for raw values from each grid are given in Table 1.

Table 1. Summary Statistics for ARCSS Grids by Physiographic Province

Site	n	Mean, cm	s.d., cm	Max, cm	Min, cm	Correlation Coefficient
			Coastal Plain			
Barrow						
Aug. 27, 1995	121	34.5	7.5	65	21	
Aug. 18, 1996	119	35.6	8.5	68	19	0.92
Atqasuk						
Aug. 30, 1995	107	44.4	19.6	100	23	
Aug. 20, 1996	107	47.2	22.6	119	23	0.94
West Dock						
Aug. 24, 1995	108	51.4	12.8	95	27	
Aug. 14, 1996	110	54.9	13.2	95	31	0.94
Betty Pingo						
Aug. 23, 1995	102	54.7	19.1	103	30	
Aug. 13, 1996	106	55.0	18.5	100	32	0.97
			Foothills			
Happy Valley						
Aug. 19, 1995	117	42.6	8.9	67	26	
Aug. 16, 1996	117	43.4	9.4	76	26	0.67
Toolik Lake						
Aug. 13, 1995	106	45.1	13.4	77	15	
Aug. 17, 1996	102	46.6	10.5	78	28	0.60
Imnavait Creek						
Aug. 20, 1995	106	49.0	9.0	72	26	
Aug. 17, 1996	111	45.9	7.9	64	25	0.31

3. Spatial Autocorrelation Analysis

3.1. Measures of Spatial Association

Little has been done to assess the interannual variability of the active layer, particularly from a spatial-analytic perspective. Persistence of characteristic patterns of thaw depth through a spatial time series could indicate the existence of highly localized controls related to land cover, terrain, and/or subsurface characteristics.

Because spatial data usually violate the assumption of independence between observations required by most applications of classical inferential statistics, statistical inference based on procedures such as element-by-element correlation between spatial fields is generally inadvisable. Many alternative methods designed specifically for spatial data have been developed, however; one of the most versatile suites of statistical techniques is spatial autocorrelation analysis, a two-dimensional extension of procedures employed in time series analysis. Developed by *Moran* [1950], generalized by *Cliff and Ord* [1973, 1981], and used widely in geography [e.g., *Chou*, 1991] and biology [e.g., *Sokal and Wartenberg*, 1983], spatial autocorrelation procedures are effective for detecting, categorizing, and quantifying spatial structure that may not be apparent from standard graphical or statistical procedures.

First-order analysis involves assessing the presence and strength of autocorrelation between neighboring elements in a geographical mesh of data values. The most commonly used index of spatial autocorrelation is Moran's I, a weighted, product-moment type correlation coefficient given by

$$I = \left(n \sum_{i=1}^{n} \sum_{j=1}^{n} w_{ij} z_i z_j \right) \Big/ \left(S_0 \sum_{i=1}^{n} z_i^2 \right) \qquad (1)$$

where n is the number of sample points (often arranged on a rectangular lattice), i and j range from 1 to n ($i \neq j$), z_i and z_j are the deviations of values at individual points from their mean value, w_{ij} is the weight given to the connection (join) between points i and j, and S_0 is the sum of the weighting matrix ($i \neq j$). The monograph by *Cliff and Ord* [1981] provides a review of the many joining and weighting schemes available for this type of analysis.

Under the commonly used assumption of randomization ("assumption R"), observations are considered to have been drawn randomly and independently from a population (or set

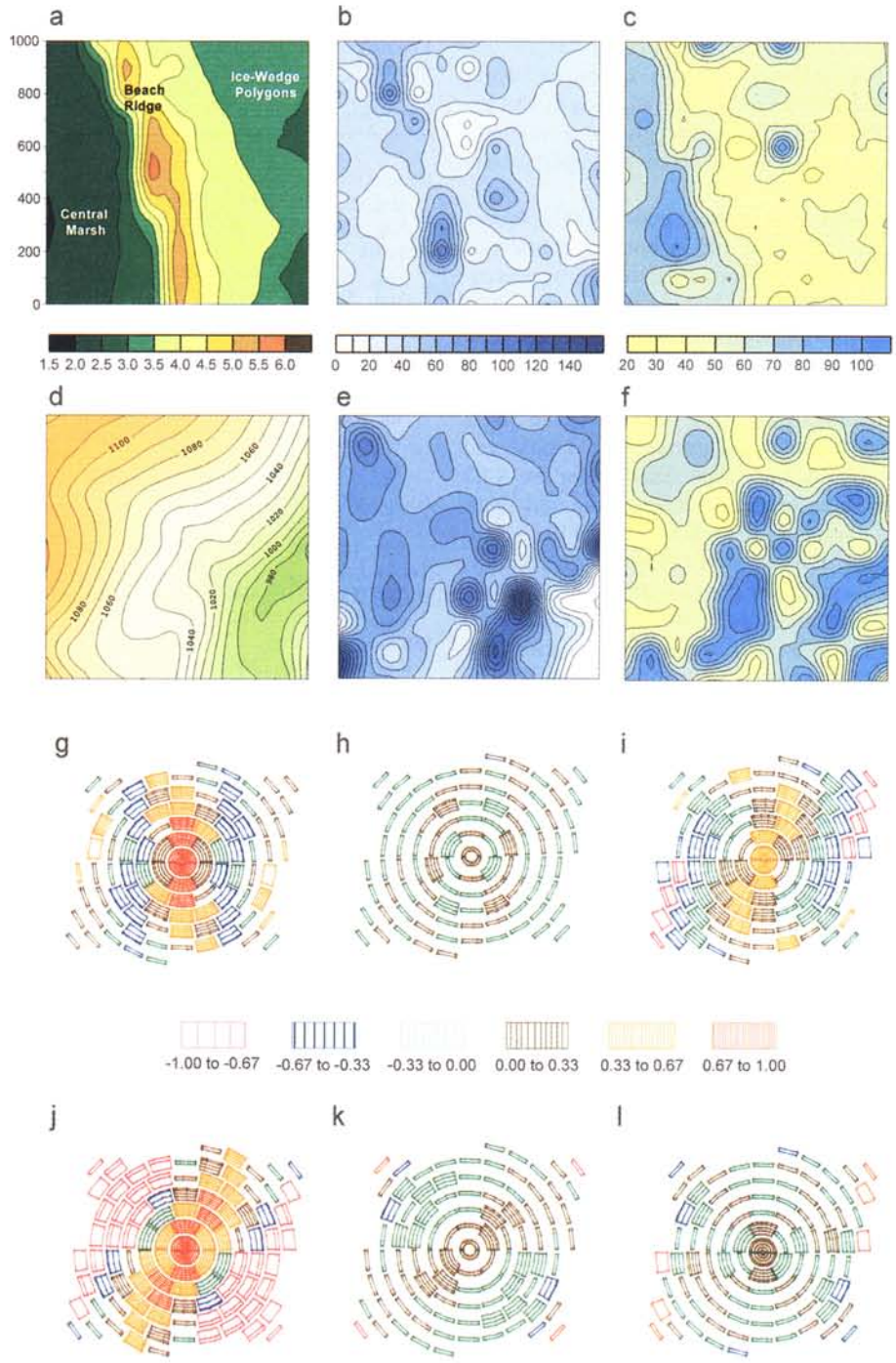

Plate 1. Maps and correlograms for 1 km^2 ARCSS grids at Barrow and Happy Valley. Scale is given in meters along left margin of first panel. All maps in Plates 1 and 2 are oriented with north at top. (a) Barrow topography (legend indicates elevation in meters above sea level (asl); (b) Barrow snow depth (centimeters), early-May 1996; (c) Barrow soil moisture (percent by volume), mid-August 1996; (d) Happy Valley topography (contour labels in meters asl); (e) Happy Valley snow depth, early-May 1995; (f) Happy Valley soil moisture, mid-August 1996. Correlograms: (g) Barrow topography; (h) Barrow snow depth; (i) Barrow soil moisture; (j) Happy Valley topography; (k) Happy Valley snow depth; (l) Happy Valley soil moisture. Correlograms show magnitude of Moran's I by shading density and as a spectral progression of color (yellow was replaced by brown to enhance legibility). Statistically significant segments are represented as thicker boxes. Further details are provided in text and by *Jacquez* [1991].

of populations) with unknown distribution(s) [*Cliff and Ord*, 1981, pp. 45–46]. Under R and in the absence of two-dimensional autocorrelation, expectations for the mean and variance, respectively, of Moran's I statistic are

$$E(I) = -1/(n-1) \tag{2}$$

$$E(I^2) = (n^2S_1 - nS_2 + 3S_0^2)/[S_0^2(n-1)], \tag{3}$$

where

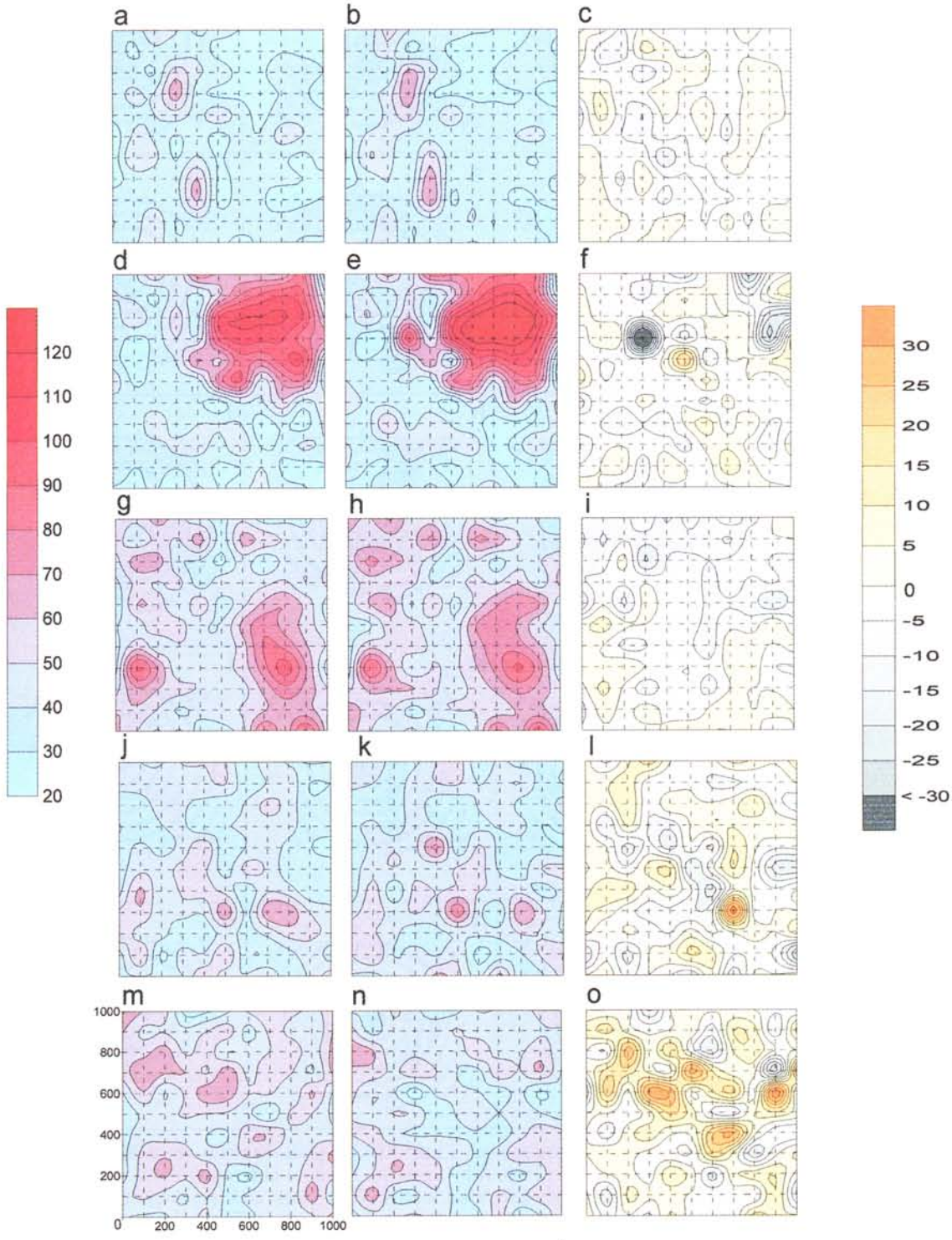

Plate 2. Maps of active-layer thickness (centimeters) on 1 km^2 ARCSS grids. Grid intersections represent locations of sampling points at 100 m intervals. Barrow grid: (a) August 27, 1995; (b) August 18, 1996; (c) difference map, based on equation (6). Atqasuk grid: (d) August 30, 1995; (e) August 20, 1996; (f) difference map. West Dock grid: (g) August 24, 1995; (h) August 14, 1996; (i) difference map. Happy Valley grid: (j) August 19, 1995; (k) August 16, 1996; (l) difference map. Imnavait Creek grid: (m) August 20, 1995; (n) August 17, 1996; (o) difference map.

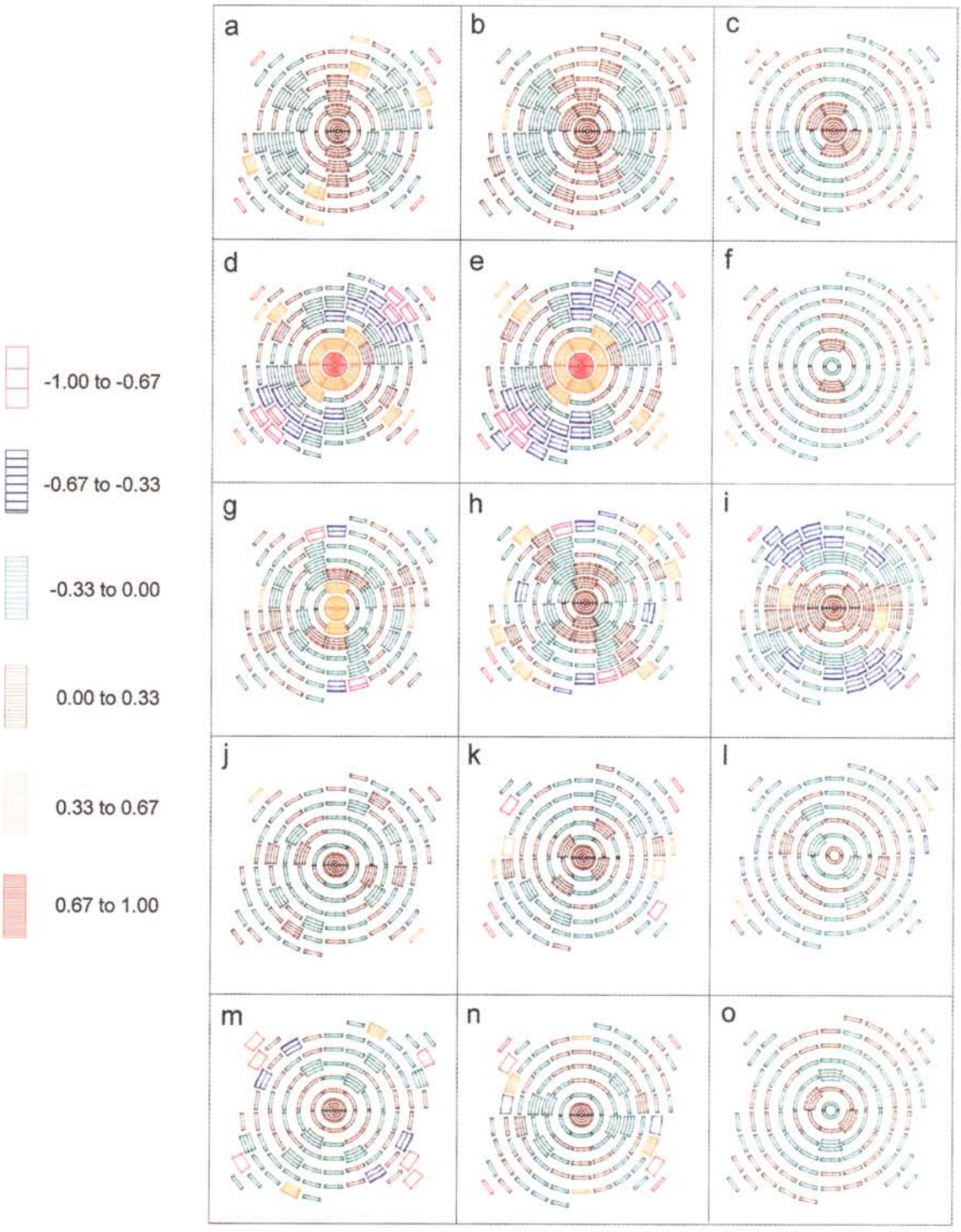

Plate 3. Correlograms for active-layer matrices from 1 km^2 ARCSS grids. Symbols are defined in Plate 1 caption and text. Barrow grid: (a) August 27, 1995; (b) August 18, 1996; (c) difference matrix. Atqasuk grid: (d) August 30, 1995; (e) August 20, 1996; (f) difference matrix. West Dock grid: (g) August 24, 1995; (h) August 14, 1996; (i) difference matrix. Happy Valley grid: (j) August 19, 1995; (k) August 16, 1996; (l) difference matrix. Imnavait Creek grid: (m) August 20, 1995; (n) August 17, 1996; (o) difference matrix.

$$S_1 = 1/2 \sum_{i=1}^{n} \sum_{j=1}^{n} (w_{ij} + w_{ji})^2 \quad (4)$$

$$S_2 = \sum_{i=1}^{n} \left(\sum_{j=1}^{n} w_{ij} + \sum_{j=1}^{n} w_{ji} \right)^2 . \quad (5)$$

Higher-order analysis compares larger spatial lags, involving progressively more distant nodes. These relationships are frequently summarized as spatial correlograms [e.g., *Cliff and Ord*, 1981, chap. 5; *Sokal and Wartenberg*, 1983], which can provide substantial insight into the scale of a spatial process. Several principles and assumptions underlie spatial autocorrelation analysis [*Sokal and Wartenberg*, 1983, p. 220], three of

which are important in the present context: (1) patterns of spatial variation produce characteristic "signatures" that can be detected by spatial autocorrelation analysis and summarized through correlograms; (2) similar signatures are produced by similar deterministic processes; and (3) changes in process or process intensity produce changes in the signatures.

Oden and Sokal [1986] developed a more sophisticated graphical method for summarizing spatial autocorrelation than the one-dimensional variety used previously. Their "directional correlograms" depict relationships involving both distance and direction, facilitating simultaneous assessment of both these fundamental spatial relationships. The correlograms are constructed as a series of segmented concentric circles ("annuli") representing successively larger distance intervals. The size and shading of circle segments correspond to the statistical significance and strength of I for specific values of distance and direction. *Oden and Sokal* [1986] provided a comprehensive guide to the construction and interpretation of directional correlograms. The procedures are implemented in a readily available software package [*Jacquez*, 1991]. Tests to assess overall statistical significance have also been developed [*Oden*, 1984] and should be applied to determine if detailed interpretation of individual correlograms is warranted [*Fortin et al.*, 1989].

3.2. Arctic System Science (ARCSS) Grids

Because thaw progression is proportional to the square root of thawing degree-day accumulation, the active layer in northern Alaska is near its maximum thickness by the middle of August. Correlograms were computed for thaw depth values observed in middle to late August 1995 and 1996 on each of the seven ARCSS grids. Weighting of the joins between nodes (equation (1)) follows a simple binary scheme in which w_{ij} is assigned a value of unity when the separation between i and j corresponds to a specified distance class, and zero otherwise. Other statistical procedures follow those outlined by *Oden and Sokal* [1986] and *Jacquez* [1991].

The correlograms employ equal-interval classes, constructed by dividing the difference between the minimum and the maximum values of I by 6, the number of classes used in the diagrams. They were first standardized by resetting extreme local values of I ($|I| > 1.0$) to 1.0 or -1.0. This operation has little overall effect because most of the affected correlogram segments involved very few pairs of points and were not statistically significant [cf. *Jong et al.*, 1984]. Larger segments of correlogram annuli (Plates 1 and 3) indicate statistically significant ($p = 0.05$) values of I in particular distance/direction classes. To enhance interpretability, all correlograms show values of Moran's I at lags of two sampling intervals.

Procedures for quantitative comparison of correlograms are not generally available. This limitation was avoided in this study because measurements were made at different times at the same general locations. Interannual variability on individual grids was evaluated by computing a "difference map" of thaw values, based on the matrix [**D**]:

$$[\mathbf{D}] = [\mathbf{Z}]_{95} - [\mathbf{Z}]_{96} \quad (6)$$

where $[\mathbf{Z}]_{95}$ and $[\mathbf{Z}]_{96}$ are the interpolated 11×11 end-of-season thaw depth matrices for individual grids in 1995 and 1996, respectively. Spatial autocorrelation measures identical to those described above were then applied to [**D**] for each location. The resulting correlograms illustrate the spatial structure of interannual differences in thaw depths. Lack of autocorrelation reflects minor, randomly distributed variations attributable to measurement error and/or small changes in probing location and provides evidence that thaw depth patterns over individual grids remain similar from year to year.

The Bonferroni procedure, which corrects for multiple comparisons [*Oden*, 1984; *Legendre and Fortin*, 1989; *Hsu*, 1996], indicates that each of the correlograms shown in Plates 1 and 3 is globally significant at the 0.05 level, except those based on interannual differences for Atqasuk, Happy Valley, Toolik Lake, and Betty Pingo, and for snow cover at Barrow. For general comparison the analysis of interannual variability was supplemented by calculation of the Pearson product-moment correlation coefficient between pairs of grid nodes for 1995 and 1996 (Table 1).

3.3. Site-Specific Analyses

3.3.1. Barrow. The Barrow grid contains three distinctive topographic units (Plate 1a), which exert strong controls over soil/vegetation/landscape relationships. Most of the eastern part of the area is upland tundra with well-defined networks of ice-wedge polygons developed in silty soils. Along the western margin is Central Marsh, a drained thaw-lake basin with wet tundra vegetation. Separating these units is a north-south trending ridge of coarse beach sediments (sands and gravels) buried at shallow depth beneath finer-grained sediments and standing 1–3 m above Central Marsh.

Because of its coastal location and cooler temperatures [*Haugen and Brown*, 1980], mean thaw depth is substantially smaller on the Barrow grid than at the other locations. End-of-summer values were very similar in 1995 and 1996. A north–south trending zone of maximum thaw (red hues) is associated with the western flank of the beach ridge (Plates 2a and 2b). The overall pattern of thaw depth mirrors topography (Plate 1a), with minimum values in the upland tundra in the east rising to maxima on the beach ridge and declining to intermediate values in Central Marsh in the west.

The 1995 and 1996 correlograms (Plates 3a and 3b) reinforce the visual impression given by the maps. The correlograms exhibit similar patterns, the dominant aspects being a north–south-oriented sequence of segments with modest but statistically significant positive autocorrelation, and segments with negative autocorrelation of similar strength in the east and west sectors. These patterns reflect the dominant topographic partitioning of the landscape within the study area. The correlation coefficient of 0.92 for the 119 paired measurements confirms the strong interannual similarity in thaw pattern and indicates that local controls over the magnitude of thaw depth persist from year to year. The difference correlogram (Plate 3c) shows modest positive autocorrelation at close lags in a north–south direction. This is an artifact of deeper thaw in 1996 in the beach ridge sediments, which are well drained and exhibit a large degree of interannual variation.

Because soil moisture has a large impact on thaw depths, the volumetric soil moisture content was measured in mid-August 1996 at each of the grid nodes using a portable Vitel Hydra-Probe®. To avoid the effects of the surface organics, a 15 cm deep plug (8 cm diameter) was removed and the probe inserted into the underlying mineral soil. The resulting map (Plate 1c) shows a general pattern of below-average (<52%) soil moisture in the upland tundra and above-average values in the thaw-lake basin. The two zones are separated by the relatively dry gravels of the beach ridge.

The maps of terrain, snow cover, soil moisture, and active-

layer thickness (Plates 1a, 1b, 1c, and 2a/2b, respectively) have similar patterns, indicating the possibility of causal links between these variables. Detailed process studies at Barrow (K. M. Hinkel, L. L. Miller, and F. E. Nelson, unpublished data, 1993–1997) indicate that snow does not exert a substantial direct effect on active-layer thickness at Barrow. Conversely, soil moisture, which is closely related to topographic position, is a major determinant of the annual maximum thaw depth. Correlograms for the elevation, snow, and soil moisture fields at Barrow (Plates 1g, 1h, and 1i, respectively) confirm these relationships. Strong similarities exist between the correlograms for thaw depth, elevation, and soil moisture, but little correspondence is apparent between these variables and snow cover, which varies at a relatively high spatial frequency.

The similarity between spatial patterns of thaw depth, soil moisture, and terrain indicates that surface hydrology, which is determined by topography, has a strong influence on the thickness of the active layer at the Barrow site. Low-lying, wet areas have enhanced thaw because water-filled soil pores have relatively high thermal conductivity. Dryer fine-textured soils have lower thermal conductivity, and large thermal gradients can be maintained in the near-surface layer. Ice lensing in the well-drained beach gravels is unlikely; the absence of pronounced latent heat effects in these coarse sediments promotes deep thaw after the frost table descends below the level of the overlying layer of finer-textured soil.

3.3.2. Atqasuk. The Atqasuk grid is located near the Meade River, approximately 100 km south of Barrow. Soils, which are developed on aeolian sands of Quaternary age, show great variability that is related closely to microtopography and drainage characteristics [*Everett*, 1980]. A large thaw-lake basin occupies the northeast quadrant of the ARCSS grid, and the terrain rises gently away from this topographic depression toward the south and west. Local relief is about 11 m. Vegetation patterns are more complex than at Barrow [*Komárková and Webber*, 1980]. Atqasuk's more continental climate and sandy substrate make a useful contrast with conditions at Barrow and elsewhere on the coastal plain.

Late-August patterns of thaw at Atqasuk for 1995 and 1996 are shown in Plates 2d and 2e. Mean thaw depths for measured grid nodes are similar in both years. Away from the influence of the lake basin, thaw depths range from 20 to 50 cm. In both years the overall range of active-layer thickness is high. The correlograms for 1995 and 1996 (Plates 3d and 3e) indicate a close relationship between terrain and thaw depth, with strong positive autocorrelation at small lags and moderate to strong negative values occurring with increasing distance. The dominant NE–SW component in the correlograms reflects a steep gradient in the thickness of the thawed layer between the drained lake basin in the northeast and the relatively small values in the upland of the southwest. These relationships provide further evidence that the primary influence over thaw variability on the coastal plain is soil moisture content, which is in turn controlled by low-frequency terrain features. Both the correlogram for the 1995/1996 difference map (Plate 3f) and the correlation coefficient of 0.94 indicate little difference in spatial pattern between 1995 and 1996, again demonstrating the importance of terrain and land cover in determining the local thickness of the active layer.

3.3.3. West Dock/Betty Pingo. The West Dock and Betty Pingo grids have relatively low relief but contain prominent, partially drained thaw-lake basins. Ice-wedge polygons are strongly in evidence on upland surfaces, and vegetation consists of moist nonacidic tundra. Within the lake basins, wet tundra and shallow water predominate. End-of-season thaw depth on the West Dock grid is shown in Plates 2g and 2h. Although a slightly greater depth of thaw occurred in 1996 (average of 55 versus 51 cm in 1995) at West Dock, visual inspection of the maps indicates that thaw patterns are similar. Prominent areas of enhanced thaw are apparent in the southern part of both maps and are associated with wetter soil conditions in the thaw-lake basins. The north–south trending band of shallow thaw near the center of the map represents higher ground separating the basins.

Moderate but statistically significant values of I near the centers of the correlograms for West Dock (Plates 3g and 3h) reflect similarities between neighboring grid nodes, an indication of internal consistency within the upland and lake basin sectors of the grid. Values of I decline rapidly at medium lags and assume statistically significant negative values along diagonal paths, an indication of strong dissimilarity between the upland and the lake basin sectors. Although not illustrated with maps, similar results were obtained from the nearby Betty Pingo site.

With minor divergences the correlograms for 1995 and 1996 indicate similar patterns of thaw on the West Dock grid, a conclusion supported by the correlation coefficient of 0.94. The large number of segments with negative autocorrelation, separated by a band of positive autocorrelation extending from west to east in the correlogram for the difference map (Plate 3i), indicates a systematic difference in the depth of thaw in parts of the map area between the two years. Close inspection of the difference map reveals a small (<10 cm) increase in active-layer thickness in the northern part of the upland in 1996, while the basins experienced similar values in 1995 and 1996. These differences may be attributable to subtle differences in soil moisture patterns in the two years.

3.3.4. Happy Valley/Toolik Lake. The Happy Valley site, located in the Arctic Foothills physiographic province, is dominated by moist acidic tussock tundra developed atop glacial till [*Auerbach et al.*, 1996]. In distinct contrast to grids on the coastal plain the Happy Valley grid encompasses rolling topography with substantial relief (Plate 1d). The terrain is oriented along a roughly northeast–southwest axis, upon which are superimposed shrubby water tracks aligned normal to the primary topographic orientation. The correlogram for topography at Happy Valley (Plate 1j) summarizes the relatively simple terrain geometry at this site very effectively. More correspondence is apparent between the map and the correlogram for snow cover at Happy Valley (Plates 1e and 1k) than for Barrow; this is apparently a consequence of the interaction between wind and topography, with larger accumulations in the valley bottom and deflation at higher elevations. Soil moisture (Plates 1f and 1l) follows a similar pattern, with dissimilarities tied to topographic position. The large number of localized closed isarithms in Plates 1e and 1f indicates that a substantial amount of variation occurs at distances smaller than the separation between sampling points.

The local variability of thaw depth is extremely high at Happy Valley. Although average thaw depth in the two years is identical (43 cm), the mapped patterns of active-layer thickness indicate that variation occurs at much higher spatial frequencies than in the coastal plain locations. Point-to-point correlation is also substantially lower than those for grids on the coastal plain (Plates 2j and 2k, Table 1). Differences between duplicate measurements made at grid nodes were large, averaging 6 cm but ranging up to 26 cm over lateral distances

of 2 m. The high-frequency variation in the active-layer maps is attributable to two sources: imperfect alignment between grid rows and water courses and the high variability of thaw depth in tussock tundra.

The water tracks at Happy Valley drain into a perennial stream in the southeast corner of the grid. Active-layer thickness is at a maximum in these wet lineations. This pattern is detected in the correlograms (Plates 3j and 3k), which show a discontinuous band of statistically significant segments with positive autocorrelation aligned in a direction corresponding to the orientation of the water tracks. The fragmented quality of this band reflects the coarse sampling interval; although grid rows are aligned roughly parallel with the water tracks, several of the widely spaced nodes do not coincide with their local positions. A similar pattern is discernible in the correlogram for soil moisture (Plate 1l). Tundra tussocks also exert considerable influence on the flow of heat to depth [*Mueller*, 1996], and some variation over very short distances can be expected on this basis. Because intertussock distances are much smaller than the sampling interval, this source of variation imparts some random appearance to the maps. Similar results were obtained from the Toolik Lake grid.

These factors indicate that at this location the 100 m spacing is inappropriate for capturing the spatial variability of active-layer thickness. A nested, hierarchical sampling scheme employed in 1996 to formally assess the scale of variability indicated that unlike sites on the coastal plain, maximum variability occurs over distances of only 1–30 m within the Happy Valley grid [*Nelson et al.*, 1997a]. The correlogram for 1995/1996 differences (Plate 3l) supports this inference. The test for global significance failed to reach the critical value, and the few segments with relatively strong values of I are scattered throughout the correlogram.

3.3.5. Imnavait Creek. The Imnavait Creek grid, also located in the Arctic Foothills, contains wet tundra at lower elevations and moist acidic tussock tundra on hillcrests and slopes [*Walker and Walker*, 1996]. The site is underlain by glacial till. The valley bottom is broad and wet, with a perennial stream trending north–south in the western portion of the map. Several prominent water tracks occupy hillslopes.

Mean thaw depth was similar in 1995 and 1996 (49 versus 46 cm). The maps (Plates 2m, 2n, and 2o) and the correlation coefficient (0.31) indicate that interannual thaw patterns are less similar than on the other grids. As with Happy Valley, the correlograms for Imnavait Creek (Plates 3m, 3n, and 3o) show much less spatial structure than those for the grids located on the coastal plain. This situation appears to be related to the mismatch between the sampling interval and the scale of active-layer variability. Although our field observations indicated that, as is the case on the other grids, enhanced thaw is associated with the water tracks and the stream valley bottom, the 100 m spacing of the grid nodes is much too large to resolve either the effects of these lineations or the high-frequency variations in tussock tundra. As at Happy Valley and Toolik Lake, a nested hierarchical sampling design [*Nelson et al.*, 1997a] indicated that maximum variability of active-layer thickness at the Imnavait Creek site is associated with small horizontal distances (1–30 m).

4. Discussion

Climatologically, the summers of 1995 and 1996 were very similar throughout the study area. Mean values of thaw over the grids were also similar in the two years. Patterns of thaw depth obtained with the systematic sampling design were spatially and temporally coherent at sites on the coastal plain but diverged substantially from those in the foothills. Continued monitoring will indicate whether some or all of these relations persist in years with markedly different climatological characteristics.

Results from the grids on the coastal plain demonstrate the effectiveness of spatial autocorrelation analysis for revealing structure in maps of active-layer thickness, as well as for illustrating subtle interannual differences. The spatial patterns are established early in the thaw season. Low-frequency topographic variation, related primarily to drained or partially drained thaw lake basins, exerts the major control over surface hydrology and soil moisture and has strong influence on the local thickness of the active layer [*Nelson et al.*, 1997a, b]. Results from the foothill sites provide indirect evidence that microscale and mesoscale topography exert an important control over thaw depth, although very substantial variations also occur at scales involving areas much larger than the grids [*Nelson et al.*, 1997b].

Data collected from the 1 km^2 grids raise a cautionary note about the necessity for reconnaissance work to determine the scale(s) at which large variability exists, prior to large investments of time and effort in detailed field work. They also highlight the dangers of extrapolating results based on point measurements to larger regions, particularly in complex terrain. Although the advent of small, inexpensive data loggers has ameliorated problems of extrapolating near-surface temperature measurements [*Nelson et al.*, 1997b], labor and capital-intensive undertakings such as instrumented boreholes will remain few in number for the foreseeable future. It is imperative that these resources be established at locations that are representative of dominant or "average" conditions. A carefully designed program of spatial sampling can help to identify such sites.

The thickness of the active layer is typically modeled as a function of air temperature. Over the 1 km^2 grids this value should be fairly uniform, and as a first approximation, the depth of thaw might also be expected to show uniformity. The patterns of thaw over the grids in 1995 and 1996 demonstrate that local conditions are important determinants of the spatial pattern and scale of active-layer thickness. Because it influences microclimate, hydrology, soil moisture, and vegetation, topography exerts a strong control over thaw patterns at several scales.

5. Conclusions

The ARCSS grids represent an attempt to establish a semipermanent network of observation sites for use in a wide range of physical and ecological investigations. Such networks have considerable potential for advancing systems science. However, the active-layer data demonstrate a danger inherent in a "one size fits all" approach to integrated science: the geometry and scale of the observation network may be suitable for one type of investigation but highly inappropriate for others.

Pronounced variations in thaw depth occur over short lateral distances on each of the ARCSS grids. The density, geographic scale, and geometry of these variations is very different in the Arctic Coastal Plain and Arctic Foothills physiographic provinces. The regular 100 m spacing employed on the grids is adequate to capture the primary scale of spatial variability on

the coastal plain, which is controlled by low-frequency, relatively equidimensional physiographic features (drained thaw-lake basins). In the foothills the 100 m spacing fails to resolve high-frequency variations (tussock tundra) or those with linear geometries (water tracks). These considerations dictate that reconnaissance sampling should be carried out in the initial stages of investigations to determine the appropriate sampling scale(s) for particular variables [e.g., *Fortin et al.*, 1989; *Webster and Oliver*, 1990; *Nelson et al.*, 1997a].

Because decomposition and microbial respiration and hence the flux of trace gases are tied closely to active-layer thickness, it follows that investigations centered on these topics should adopt similar sampling designs. Systematic sampling strategies are relatively easy to implement in the field, but the node spacing required to resolve spatial patterns varies inversely with the spatial heterogeneity of the phenomenon of interest. In the foothills a fixed-interval design sufficient to resolve the scale of maximum variability on the 1 km^2 grids would require far more effort than could reasonably be expended. Other methods, such as hierarchical sampling and analysis [*Webster and Oliver*, 1990; *Walker and Walker*, 1991] or stratification by land cover category [*Nelson et al.*, 1997b; *Muller et al.*, 1998], should be used to assess spatial variability in such situations. Given the large number of sample points on the ARCSS grids, however, the 100 m spacing appears adequate to obtain summary statistics that can be used to track long-term changes in active-layer thickness for the entire area [*Fagan*, 1995].

Spatial analysis can play an important role in climate change investigations. This study has demonstrated that two-dimensional correlograms are capable of detecting subtle interannual variations in active-layer thickness. In combination with knowledge about terrain and hydrologic characteristics in the study area these procedures can be used to infer processes responsible for the changes, as at the West Dock site. If repeated over a series of years, analysis of spatial time series may be capable of discerning between this kind of interannual variability and gradual changes related to more fundamental, climate-induced change. The CALM program was established to create long-term records of active-layer thickness at sites representative of zonal land cover and edaphic conditions. Applied over the long term to a large number of sites, spatial analytic techniques may help to discern between short- and long-term changes in the active layer.

Acknowledgments. This research was supported by National Science Foundation grants OPP-9318528 and OPP-9612647 (FEN) and SES-9308334 and OPP-9529783 (KMH). We thank the Polar Ice Coring Office (Lincoln, Nebraska), the Barrow Environmental Observatory, and Sally Marsh (SUNY-Albany) for logistical support and administrative services. Constructive comments from A. G. Lewkowicz and two anonymous reviewers led to numerous improvements in the paper.

References

Anisimov, O. A., N. I. Shiklomanov, and F. E. Nelson, Effects of global warming on permafrost and active-layer thickness: Results from transient general circulation models, *Global Planet. Change*, *15*, 61–77, 1997.

Auerbach, N. A., D. A. Walker, and J. Bockheim, Land cover of the Kuparuk River Basin, Alaska (map scale 1:500,000), Joint Facil. for Reg. Ecosyst. Anal., Univ. of Colo., Boulder, 1996.

Brown, J., A. E. Taylor, F. E. Nelson, and K. M. Hinkel, The Circumpolar Active Layer Monitoring (CALM) program: Structure and current status, in *Abstracts of the 27th Arctic Workshop*, p. 25, Dep. of Geogr., Univ. of Ottawa, Ottawa, 1997.

Chou, Y. H., Map resolution and spatial autocorrelation, *Geogr. Anal.*, *23*, 228–246, 1991.

Cliff, A. D., and J. K. Ord, *Spatial Autocorrelation*, Pion, London, 1973.

Cliff, A., and J. Ord, *Spatial Processes, Models and Applications*, Pion, London, 1981.

Cubasch, U., K. Hasselmann, H. Hock, E. Maier-Reimer, B. D. Santer, and R. Sausen, Time-dependent greenhouse warming computations with a coupled ocean-atmosphere model, *Clim. Dyn.*, *8*, 55–69, 1992.

de Jong, P., C. Sprenger, and F. van Veen, On extreme values of Moran's I and Geary's c, *Geogr. Anal.*, *16*, 17–24, 1984.

Dutton, E. G., and D. J. Endres, Date of snowmelt at Barrow, Alaska, U.S.A., *Arc. Alp. Res.*, *23*, 115–119, 1991.

Evans, B. M., D. A. Walker, C. S. Benson, E. A. Nordstrand, and G. W. Peterson, Spatial interrelationships between terrain, snow distribution and vegetation patterns at an Arctic foothills site in Alaska, *Holarc. Ecol.*, *12*, 270–278, 1989.

Everett, K. R., Distribution and variability of soils near Atkasook, Alaska, *Arc. Alp. Res.*, *12*, 433–446, 1980.

Fagan, J. D., Sampling designs for the measurement of active-layer thickness, M.S. thesis, Rutgers Univ., New Brunswick, N. J., 1995.

Fortin, M. J., P. Drapeau, and P. Legendre, Spatial autocorrelation and sampling design in plant ecology, *Vegetatio*, *83*, 209–222, 1989.

Goodrich, L. E., The influence of snow cover on the ground thermal regime, *Can. Geotech. J.*, *19*, 421–432, 1982.

Hastings, S. J., S. A. Luchessa, W. C. Oechel, and J. D. Tenhunen, Standing biomass and production in water drainages of the foothills of the Phillip Smith Mountains, *Holarc. Ecol.*, *12*, 304–311, 1989.

Haugen, R. K., Climate of remote areas in north-central Alaska: 1975–1979 summary, *CRREL Rep.*, *82-35*, 1–110, 1982.

Haugen, R. K., and J. Brown, Coastal-inland distributions of summer air temperature and precipitation in northern Alaska, *Arc. Alp. Res.*, *12*, 403–412, 1980.

Haugen, R. K., J. Brown, and T. A. May, Climatic and soil temperature observations at Atkasook on the Meade River, Alaska, summer 1975, *CRREL Spec. Rep.*, *76-1*, 1–25, 1976.

Hinkel, K. M., and J. R. J. Nicholas, Active layer thaw rate at a boreal forest site in central Alaska, U.S.A., *Arc. Alp. Res.*, *27*(1), 72–80, 1995.

Hinkel, K. M., S. I. Outcalt, and F. E. Nelson, Near-surface summer heat-transfer regimes at adjacent permafrost and non-permafrost sites in central Alaska, in *Proceedings of the Sixth International Conference on Permafrost*, vol. 1, pp. 261–266, South China Univ. of Technol. Press, Wushan Guangzhou, China, 1993.

Hinzman, L. D., and D. L. Kane, Potential response of an arctic watershed during a period of global warming, *J. Geophys. Res.*, *97*, 2811–2820, 1992.

Hsu, J. C., *Multiple Comparisons: Theory and Methods*, Chapman and Hall, New York, 1996.

Jacquez, G. M., *C2D: Spatial Autocorrelation in Two Dimensions*, Exeter Publishing, Setauket, N. Y., 1991.

Jumikis, A. R., *Thermal Geotechnics*, Rutgers Univ. Press, New Brunswick, N. J., 1977.

Komárková, V., and P. J. Webber, Two low Arctic vegetation maps near Atkasook, Alaska, *Arc. Alp. Res.*, *12*, 447–472, 1980.

Legendre, P., and M.-J. Fortin, Spatial pattern and ecological analysis, *Vegetatio*, *80*, 107–138, 1989.

Leverington, D. W., and C. R. Duguay, Evaluation of three supervised classifiers in mapping "depth to late-summer frozen ground," central Yukon Territory, *Can. J. Remote Sens.*, *22*, 163–174, 1996.

Mackay, J. R., Probing for the bottom of the active layer, *Geol. Surv. Can. Pap.*, *77-1A*, 327–328, 1977.

Mackay, J. R., Active layer changes (1968 to 1993) following the forest-tundra fire near Inuvik, N.W.T., Canada, *Arc. Alp. Res.*, *27*, 323–336, 1995.

Manabe, S., R. J. Stouffer, M. J. Spelman, and K. Bryan, Transient responses of a coupled ocean-atmosphere model to gradual changes of atmospheric CO_2, I, Annual mean response, *J. Clim.*, *4*, 785–818, 1991.

McMichael, C. E., A. S. Hope, D. A. Stow, and J. B. Fleming, The relation between active layer depth and a spectral vegetation index in arctic tundra landscapes of the North Slope of Alaska, *Int. J. Remote Sens.*, *18*, 2371–2382, 1997.

Moran, P. A. P., Notes on continuous stochastic phenomena, *Biometrika*, *37*, 17–23, 1950.

Mueller, G. R., A multiscale GIS analysis of active layer thickness and

vegetation type on Alaska's North Slope, M.A. thesis, State Univ. of N. Y., Albany, 1996.

Muller, S. V., D. A. Walker, F. Nelson, N. A. Auerbach, J. Bockheim, S. Guyer, and D. Sherba, Accuracy assessment of a landcover map of the Kuparuk River basin, Alaska, *Photogramm. Eng. and Remote Sens.*, in press, 1998.

Murphy, J. M., and J. F. B. Mitchell, Transient response of the Hadley Centre coupled model to increasing carbon dioxide, II, Spatial and temporal structure of response, *J. Clim.*, *8*, 57–80, 1994.

Nelson, F., J. Brown, A. Lewkowicz, and A. Taylor, Active layer protocol, in *ITEX Manual*, 2nd ed., edited by U. Molau, and P. Molgaard, pp. 14–16, Int. Tundra Exp., Copenhagen, 1996.

Nelson, F. E., A. H. Lachenbruch, M.-K. Woo, E. A. Koster, T. E. Osterkamp, M. K. Gavrilova, and G. D. Cheng, Permafrost and changing climate, in *Proceedings of the Sixth International Conference on Permafrost*, vol. 2, pp. 987–1005, South China Univ. of Technol. Press, Wushan, Guangzhou, China, 1993.

Nelson, F. E., G. R. Mueller, and N. I. Shiklomanov, Sampling designs for assessing variability of active-layer thickness, in *Abstracts, 93rd AAG Annual Meeting*, p. 191, Assoc. of Am. Geogr., Washington, D. C., 1997a.

Nelson, F. E., N. I. Shiklomanov, G. Mueller, K. M. Hinkel, D. A. Walker, and J. G. Bockheim, Estimating active-layer thickness over a large region: Kuparuk River basin, Alaska, U.S.A., *Arc. Alp. Res.*, *29*, 367–378, 1997b.

Oden, N. L., Assessing the significance of a spatial correlogram, *Geogr. Anal.*, *16*, 1–16, 1984.

Oden, N. L., and R. R. Sokal, Directional autocorrelation: An extension of spatial correlograms to two dimensions, *Syst. Zool.*, *35*, 608–617, 1986.

Peddle, D. R., and S. E. Franklin, Classification of permafrost active layer depth from remotely sensed and topographic evidence, *Remote Sens. Environ.*, *44*, 67–80, 1993.

Reynolds, J. F., and J. D. Tenhunen (eds.), *Landscape Function and Disturbance in Arctic Tundra*, Springer-Verlag, New York, 1996.

Savtchenko, V. (Ed.), *Proceedings of a Meeting of Experts on Cryosphere and Climate, Cambridge, U.K., 2–4 February 1997*, World Clim. Res. Programme/World Meteorol. Organ., Geneva, 1998.

Smith, M. W., Microclimatic influences on ground temperatures and permafrost distribution, Mackenzie Delta, Northwest Territories, *Can. J. Earth Sci.*, *12*, 1421–1438, 1975.

Smith, W. H. F., and P. Wessel, Gridding with continuous curvature splines in tension, *Geophysics*, *55*, 293–305, 1990.

Sokal, R. R., and D. E. Wartenberg, A test of spatial autocorrelation using an isolation by distance model, *Genetics*, *105*, 219–237, 1983.

Waelbroeck, C., Climate-soil processes in the presence of permafrost: A systems modelling approach, *Ecol. Modell.*, *69*, 185–225, 1993.

Waelbroeck, C., P. Monfray, W. C. Oechel, S. Hastings, and G. Vourlitis, The impact of permafrost thawing on the carbon dynamics of tundra, *Geophys. Res. Lett.*, *24*, 229–232, 1997.

Wahrhaftig, C., Physiographic divisions of Alaska, *USGS Prof. Pap. 482*, 52 pp., U.S. Geol. Surv., Washington, D. C., 1965.

Walker, D. A., Arctic Alaskan vegetation disturbance and recovery: A conceptual framework for the issue of cumulative impacts, in *Disturbance and Recovery in Arctic Lands: An Ecological Perspective*, edited by R. M. M. Crawford, pp. 457–480, Kluwer Acad., Norwell, Mass., 1997.

Walker, D. A., and M. D. Walker, History and pattern of disturbance in Alaskan arctic terrestrial ecosystems: A hierarchical approach to analysing landscape change, *J. Appl. Ecol.*, *28*, 244–276, 1991.

Walker, D. A., and M. D. Walker, Terrain and vegetation of the Imnavait Creek watershed, in *Landscape Function and Disturbance in Arctic Tundra, Ecological Studies*, edited by J. F. Reynolds, and J. D. Tenhunen, pp. 73–108, Springer-Verlag, New York, 1996.

Walker, D. A., E. Binnian, B. M. Evans, N. D. Lederer, E. Nordstrand, and P. J. Webber, Terrain, vegetation and landscape evolution of the R4D research site, Brooks Range foothills, Alaska, *Holarc. Ecol.*, *12*, 238–261, 1989.

Webster, R., and M. A. Oliver, *Statistical Methods in Soil and Land Resource Survey*, Oxford Univ. Press, New York, 1990.

Weller, G., and B. Holmgren, The microclimates of the Arctic tundra, *J. Appl. Meteorol.*, *13*, 854–862, 1974.

Weller, G., F. S. Chapin, K. R. Everett, J. E. Hobbie, D. Kane, W. C. Oechel, C. L. Ping, W. S. Reeburgh, D. Walker, and J. Walsh, The Arctic Flux Study: A regional view of trace gas release, *J. Biogeogr.*, *22*, 365–374, 1995.

Williams, P. J., Permafrost and climate change: Geotechnical implications, *Philos. Trans. R. Soc. London, Ser. A*, *352*, 347–358, 1995.

Zhang, T., T. E. Osterkamp, and K. Stamnes, Some characteristics of the climate in northern Alaska, U.S.A., *Arc. Alp. Res.*, *28*, 509–518, 1996a.

Zhang, T., K. Stamnes, and S. A. Bowling, Impact of clouds on surface radiative fluxes and snowmelt in the Arctic and Subarctic, *J. Clim.*, *9*, 2110–2123, 1996b.

F. E. Nelson, G. R. Mueller, and N. I. Shiklomanov, Department of Geography, University of Delaware, Newark, DE 19716.

K. M. Hinkel and L. L. Miller, Department of Geography, University of Cincinnati, Cincinnati, OH 45221.

D. A. Walker, Institute of Arctic and Alpine Research, University of Colorado, Boulder, CO 80309.

(Received August 8, 1997; revised February 11, 1998; accepted February 12, 1998.)